Journal of Nuclear Materials 385 (2009) 400–406

Contents lists available at ScienceDirect

Journal of Nuclear Materials

journal homepage: www.elsevier.com/locate/jnucmat

Preparation, sintering and leaching of optimized uranium thorium dioxides

N. Hingant [a], N. Clavier [a,b,*], N. Dacheux [a,b], N. Barre [a], S. Hubert [a], S. Obbade [c], F. Taborda [a], F. Abraham [c]

[a] Groupe de Radiochimie, IPNO – UMR 8608 CNRS/UPS-11, Univ. Paris-Sud-11, 91406 Orsay, France
[b] ICSM – UMR 5257 CNRS/CEA/UM2/ENSCM, Centre de Marcoule, BP 17171, 30207 Bagnols/Cèze, France
[c] UCCS – UMR 8181, ENSCL/USTL, Bât. C7, BP 90108, 59652 Villeneuve d'Ascq cedex, France

ARTICLE INFO

PACS:
28.41.Vx
81.20.Ev
82.45.Bb
81.16.Be
81.05.Je
81.20.Fw

ABSTRACT

Mixed actinide dioxides are currently studied as potential fuels for several concepts associated to the fourth generation of nuclear reactors. These solids are generally obtained through dry chemistry processes from powder mixtures but could present some heterogeneity in the distribution of the cations in the solid. In this context, wet chemistry methods were set up for the preparation of $U_{1-x}Th_xO_2$ solid solutions as model compounds for advanced dioxide fuels. Two chemical routes of preparation, involving the precipitation of crystallized precursor, were investigated: on the one hand, a mixture of acidic solutions containing cations and oxalic acid was introduced in an open vessel, leading to a poorly-crystallized precipitate. On the other hand, the starting mixture was placed in an acid digestion bomb then set in an oven in order to reach hydrothermal conditions. By this way, small single-crystals were obtained then characterized by several techniques including XRD and SEM. The great differences in terms of morphology and crystallization state of the samples were correlated to an important variation of the specific surface area of the oxides prepared after heating, then the microstructure of the sintered pellets prepared at high temperature. Preliminary leaching tests were finally undertaken in dynamic conditions (i.e. with high renewal of the leachate) in order to evaluate the influence of the sample morphology on the chemical durability of the final cohesive materials.

1. Introduction

Several actinide-based materials, including oxides, carbides or nitrides, are currently studied as potential fuels for the future generations of nuclear reactors [1]. Among them, actinides mixed dioxides are already successfully employed in the PWR's and are envisaged in several Gen-III and Gen-IV concepts [2–4]. Consequently, several physico-chemical properties of the mixed dioxides, such as the cationic distribution in the structure, should be optimized in order to fit with the high pressures and temperatures generated in such reactors [5]. The development of a sustainable fuel cycle also imposes to control the spent fuel management, either in the field of reprocessing or in the case of a direct storage.

Mixed actinide dioxides fuels (such as $Pu_{1-x}U_xO_2$, MOx) are currently prepared through dry chemistry routes based on pyrometallurgy processes. Nevertheless, it could result in some heterogeneity in the distribution of the cations in the structure [6]. The preparation of $U_{1-x}Th_xO_2$ model compounds was thus undertaken *via* wet chemistry methods, involving the precipitation of crystallized precursors [7], as a model for the forthcoming synthesis of Pu/Th, Np/Th or Pu/U compounds. Among the methods usually considered, the use of hydrothermal conditions is expected to provide several benefits, starting with the precipitation of low-temperature crystallized precursors, especially in the field of an improvement in the sintering capability as well as in the homogeneity of the distribution of the cations in the structure [8].

Consequently, two different wet chemical routes were developed in order to perform the synthesis of low-temperature precursors of (U,Th) mixed dioxides. Their physico-chemical characterization was then undertaken through XRD and SEM prior to the sintering step. The densification of the pellets was followed by the means of dilatometry and SEM observations in order to establish the relationships existing between the morphology of the precursors and the properties of the final $U_{1-x}Th_xO_2$ model compounds. Finally, preliminary leaching tests were undertaken to link the densification rate and the microstructure of the pellet with the chemical durability of the mixed actinide dioxides as it was previously suggested for ThO_2 [9].

This paper gives the first insight on a more global study aiming to correlate the initial conditions of preparation of the nuclear ceramic materials with their final physico-chemical properties, such as sintering capability, chemical durability or resistance to radiation damage.

* Corresponding author. Address: Groupe de Radiochimie, IPNO – UMR 8608 CNRS/UPS-11, Univ. Paris-Sud-11, 91406 Orsay, France. Tel.: +33 4 66 33 92 08; fax: +33 4 66 79 76 11.
E-mail address: nicolas.clavier@icsm.fr (N. Clavier).

0022-3115/$ - see front matter © 2008 Elsevier B.V. All rights reserved.
doi:10.1016/j.jnucmat.2008.12.011

2. Experimental

2.1. Synthesis and characterization of the precursors

The chemical reagents were supplied by VWR, Merck and Aldrich-Fluka. Concentrated thorium chloride solution ($C \approx 1.8$ M) was issued from Rhodia while uranium chloride was obtained by dissolving uranium metal chips in 4 M hydrochloric acid. The initial actinides solutions were diluted in order to obtain a final concentration of 0.7 and 1.1 M, respectively.

Two different chemical routes were considered for the synthesis of $U_{1-x}Th_xO_2$ solid solutions, both based on the initial precipitation of crystallized precursors from a mixture of hydrochloric solutions containing the cations and oxalic acid. In the first route, called 'open system', the oxalic acid was added dropwise into the actinides solution stirred in a beaker, and heated at 323 K under ultrasonic agitation. In the second method, called 'closed system', the mixture was placed in a closed PTFE container set in a Parr acid digestion bomb then heated in an oven for a week at 403 K. In both conditions, the so-obtained precipitates were separated from the supernatant by filtration or centrifugation, washed several times with deionized water and ethanol, dried at about 343 K overnight then finally ground in an agate mortar. The expected $U_{1-x}Th_xO_2$ mixed oxide powders were finally obtained after heating above 673 K.

Electron probe microanalyses (EPMA) were carried out using a Cameca SX50 or a SX100 apparatus. Thoria ThO_2 (M_α ray of thorium) and urania $UO_{2.12}$ (M_β ray of uranium) were used as calibration standards. The X-ray powder diffraction (XRD) diagrams were collected using a Bruker AXS D8 Advance diffractometer using Cu K_α radiation ($\lambda = 1.5418$ Å). The unit cell parameters were refined using the Fullprof software [10] while average Full Width at Half Maximum (FWHM) was determined by the means of the Diffrac^{plus} EVA program, considering the five more intense diffraction rays of the pattern. SEM micrographs were obtained on a Hitachi S2500 or FEG S4800 apparatus. Finally, the oxalate to oxide transformation was followed by thermogravimetric (TG) and differential thermal (DT) analyses using a Setaram 92–16 apparatus under inert atmosphere.

2.2. Sintering procedure

The sintering of $U_{1-x}Th_xO_2$ solid solutions was performed through a two-step procedure based on a uniaxial pressing at room temperature in a tungsten carbide die followed by a heat treatment between 1673 and 1973 K. This latter was systematically performed under Ar or Ar/H_2 atmosphere in order to avoid the oxidation of tetravalent uranium. Complementary hot pressing experiments were also undertaken. In these latter conditions, several heating/pressing steps were applied to the sample up to 20 MPa and 1523 K.

The resulting relative densities were determined by water pycnometric using a Mettler-Toledo XP204 apparatus while the determination of the dimensions of the pellets led to the geometric density. Complementary studies were performed on a TMA 92 dilatometer from Setaram working under argon atmosphere from room temperature to 1773 K.

2.3. Leaching experiments

The resistance of the prepared materials to aqueous alteration was evaluated through leaching tests performed in acidic media (HNO_3) in polytetrafluoroethylene (PTFE) reactors considering high leachate renewal (called 'dynamic' experiments). The concentrations of elements released in the leachate (U,Th) were determined by Inductively Coupled Plasma Atomic Emission Spectrometry (ICP–AES) using a Jobin-Yvon Ultima or a Perkin–Elmer Optima 2000 apparatus. From these results, the normalized leaching N_L (expressed in $g \cdot m^{-2}$) and the associated normalized dissolution rate R_L (in $g \cdot m^{-2} \cdot d^{-1}$) were determined considering the following equation:

$$R_L(\mathrm{An}) = \frac{dN_L(\mathrm{An})}{dt} = \frac{d}{dt}\left(\frac{C_{\mathrm{An}} \times V \times M_{\mathrm{An}}}{f_{\mathrm{An}} \times S}\right) \approx \frac{V \times M_{\mathrm{An}}}{f_{\mathrm{An}} \times S} \times \left(\frac{dC_{\mathrm{An}}}{dt}\right) \quad (1)$$

where An = U, Th.

In this expression, C_{An} is the concentration of the actinide in the leachate (expressed in $g \cdot L^{-1}$); V, the volume of leachate; f_{An} and M_{An}, the fraction of the actinide considered in the solid and its molar mass, respectively; and S, the surface of the solid (determined from the specific surface area) [11]. Moreover, f_{An} and S are supposed to be constant during the leaching since a congruent dissolution with low normalized dissolution rates is generally observed.

3. Results and discussion

3.1. Microstructural characterization of the powdered compounds

From EPMA experiments, the powdered samples were found to be homogeneous and single-phase whatever the method of preparation considered. The elementary weight loadings as well as the mole ratios were found to be consistent with that expected even if the uranium amount was sometimes found slightly lower due to the presence of a small amount of U(VI) in the initial solution and/or to the weak oxidation of U(IV) into U(VI) during the precipitation process. In order to evaluate the influence of the preparation method on several physico-chemical properties of the precursors as well as the final dioxides, the microstructural characterization of the powdered compounds was undertaken in terms of crystallization state (XRD), morphology (SEM) and specific surface area (N_2 adsorption-BET method).

3.1.1. XRD results

The structure of the compounds precipitated at low temperature for various Th/(Th + U) mole ratios (i.e. $x = 0.50$, 0.75 and 1.00) was determined from their XRD pattern (Fig. 1(A)). All the XRD lines observed were assigned to the orthorhombic *Ccca* structure already reported for the uranium (IV) oxalate dihydrate ($U(C_2O_4)_2 \cdot 2H_2O$) by Duvieubourg-Garela et al. [12]. Also, the best crystallization state was obtained for the precursors prepared under hydrothermal conditions (average FWHM of less than 0.1° versus 0.2° for the 'open system', which nearly corresponds to the resolution of the XRD diffractometer). The very good accuracy of the peak positions allowed to refine the unit cell parameters of the (U,Th) mixed oxalates. According to the Vegard's law [13], the linear variation of the a, b and c parameters and associated unit cell volume versus the substitution rate, x, (Fig. 1(B)) indicates the formation of a continuous $U_{1-x}Th_x(C_2O_4)_2 \cdot 2H_2O$ solid solution between the Th- and U-end-members (Table 1). It is worth to note that only the c parameter is significantly affected by the replacement of thorium by uranium in the structure. In these conditions, the increase of the unit cell volume is associated to the deformation of the layer geometry due to the smaller ionic radius of uranium (1.08 Å [14]) compared to thorium (1.13 Å) in the ten-fold coordination.

3.1.2. SEM

The best crystallization state of the oxalate precursors obtained through the 'closed system' was confirmed during the SEM obser-

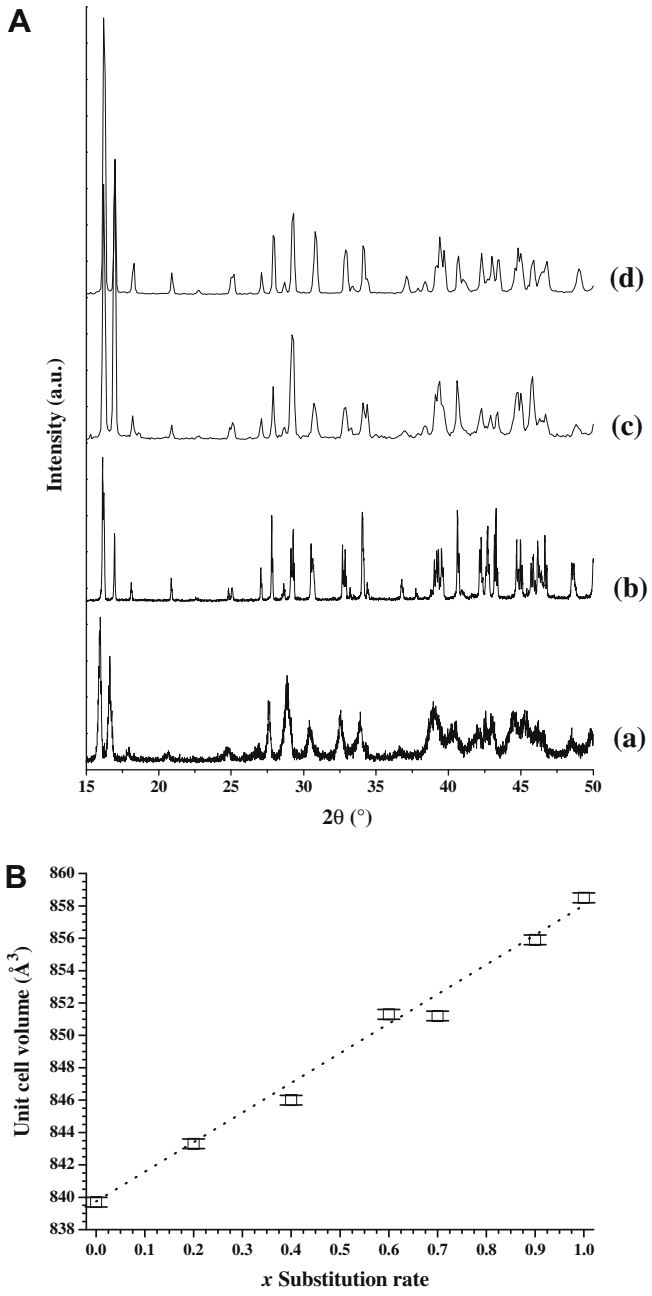

Fig. 1. (A) XRD patterns of $Th(C_2O_4)_2 \cdot 2H_2O$ prepared in 'open' system (a) and of $U_{1-x}Th_x(C_2O_4)_2 \cdot 2H_2O$ solid solutions ($x = 1.00$; 0.75; 0.50) precipitated in 'closed' system (respectively b,c,d). (B) Linear variation of the unit cell volume of $U_{1-x}Th_x(C_2O_4)_2 \cdot 2H_2O$ solid solutions versus x. The data associated to $x = 0$ correspond to that reported in [12].

Table 1
Variation of the unit cell parameters of $U_{1-x}Th_x(C_2O_4)_2 \cdot 2H_2O$ solid solutions versus x.

Lattice parameter		Unit
a	$8.457(2) + 0.005(4) \cdot x$	Å
b	$10.417(5) - 0.034(7) \cdot x$	Å
c	$9.532(12) + 0.234(16) \cdot x$	Å
V	$839.7(9) + 18.3(9) \cdot x$	Å^3

vations. Indeed, some large differences in the morphology of the powdered samples depending on the preparation method were evidenced. On the one hand, the powders precipitated in 'open system' are constituted by small grains of about 1 μm in length which aggregate to form larger square-shaped particles reaching 5–10 μm (Fig. 2(a)). On the other hand, the samples prepared in hydrothermal conditions ('closed system') appear as small single-crystals of 30 to 100 μm (Fig. 2(b)). This important difference in the grain size was correlated to the specific surface areas obtained from BET measurements. As a matter of fact, the surface area value determined for samples prepared in 'closed system' (about 0.3 $m^2 \cdot g^{-1}$) is almost one order of magnitude weaker than that of samples prepared in 'open system' (typically from 2.5 to 3.0 $m^2 \cdot g^{-1}$). The variation of the morphology and surfaces was also examined through SEM after calcination at various temperatures (see Fig. 2(c–f), respectively).

3.1.3. TG and DT analyses

The transformation of (U,Th)-oxalate into mixed dioxide was then followed versus the heating temperature by using TG/DT analyses (Fig. 3). Three steps were evidenced, corresponding to a total weight loss of 40%. First, the small weight loss of 4% around 473 K was correlated to the departure of one water molecule, leading to $U_{1-x}Th_x(C_2O_4)_2 \cdot H_2O$. Whatever the chemical composition considered, this latter tends to rehydrate in air or under moist atmosphere which underlines the structural role of this water molecule. Nevertheless, the kinetic of water readsorption was found to vary strongly with the uranium amount in the solid. The samples were then found to be fully dehydrated after heating between 533 and 593 K. Anhydrous $U_{1-x}Th_x(C_2O_4)_2$ solid solutions were found to be stable up to 633–663 K: in this range of temperature, the oxalate group decomposition yields CO and CO_2 and the corresponding actinide dioxide. Contrarily to what has been observed during the thermal decomposition study of $Pu(C_2O_4)_2 \cdot 6H_2O$ [15], the existence of carbonated or oxo-carbonated intermediates was not found in this study. This could be explained by the different redox behaviour of U(IV) compared to Pu(IV) since the formation of $Pu(C_2O_4)(CO_3)_{0.5}$ and $Pu(C_2O_4)_{0.5}(CO_3)$ was associated to the reduction of Pu(IV) in Pu(III) which redox reaction is unlikely for uranium in our operating conditions.

3.1.4. Specific surface area determination

The TG/DT study did not allow to clearly evidence the influence of the preparation conditions on the transformation temperatures. Nevertheless, it was found to strongly control the morphology of the powders when heating, especially in terms of the grain size. Indeed, the specific surface area was followed versus the heat temperature and coupled to SEM observations (Fig. 2(c–f)). For both preparation routes, a maximum in the surface area was found around 673 K. Nevertheless, the powders precipitated in hydrothermal conditions exhibited a significantly larger value (typically between 40 and 50 $m^2 \cdot g^{-1}$) compared to that prepared in 'open system' (10–15 $m^2 \cdot g^{-1}$). This difference probably comes from the strong constraint imposed in the hydrothermally formed single-crystals during the oxalate to oxide transformation. Indeed, the elimination of CO and CO_2 is probably responsible in the crumbling of the grains then in the formation of sub-micrometric particles (Fig. 2(d)).

After this drastic transformation, the increase of temperature above 673 K induces a progressive grain growth step then finally the formation of grain boundaries at high temperature (Fig. 2(e–f)). In these conditions, the specific surface area decreases for both systems down to about 1 $m^2 \cdot g^{-1}$ at 1573 K.

3.2. Sintering

Considering the changes of the powder morphology versus the heating temperature, the samples prepared during the precipitation step were first heated at 673 K for 10 h to optimize their reactivity (increase of the specific surface area), then shaped by

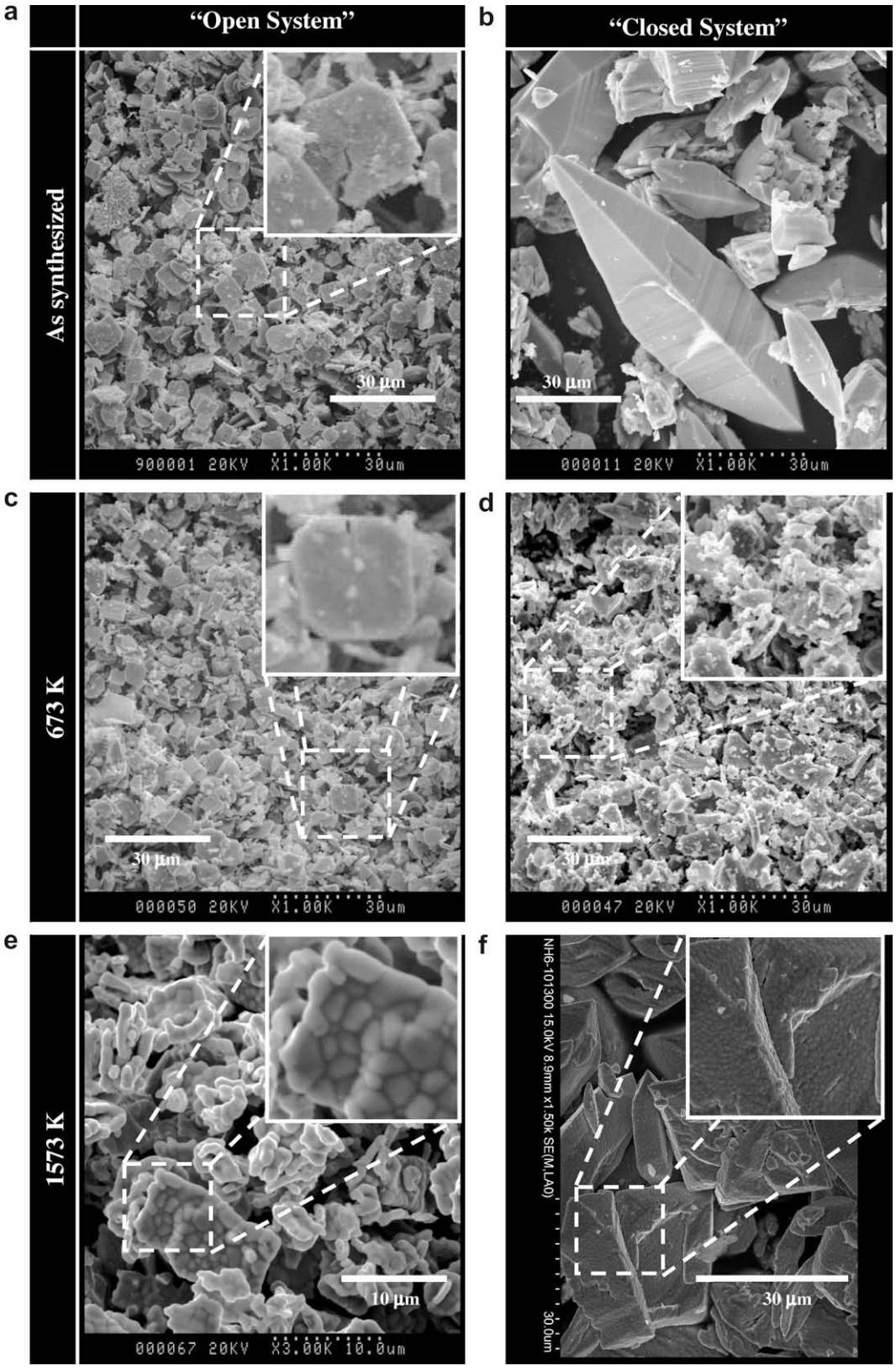

Fig. 2. SEM micrographs of $U_{0.5}Th_{0.5}(C_2O_4)_2 \cdot 2H_2O$ solid solution and corresponding $U_{0.5}Th_{0.5}O_2$ obtained after heating at 673 and 1573 K.

uniaxial pressing at room temperature (200 MPa) and finally heated at high temperature.

In order to determine the heating time and temperature required for the complete densification of the pellets, a dilatometric study was undertaken on samples prepared either in 'open' or 'closed' systems (Fig. 4) and coupled to density measurements. Whatever the method considered, the variation of the linear shrinkage appears continuous, in good agreement with the chem-

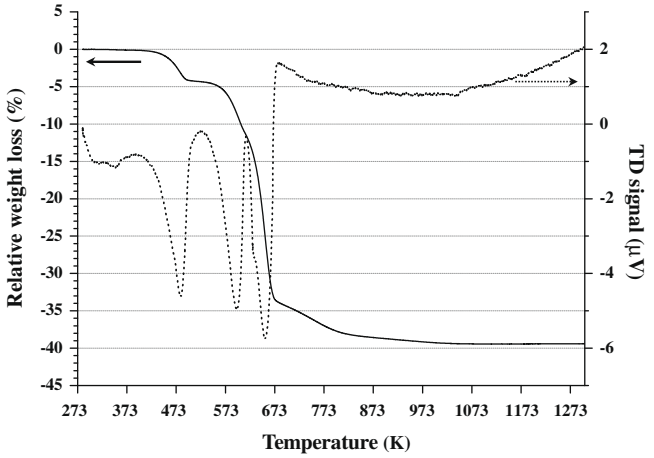

Fig. 3. TG and TD curves obtained in argon atmosphere for $U_{0.5}Th_{0.5}(C_2O_4)_2 \cdot 2H_2O$ prepared in 'closed system'.

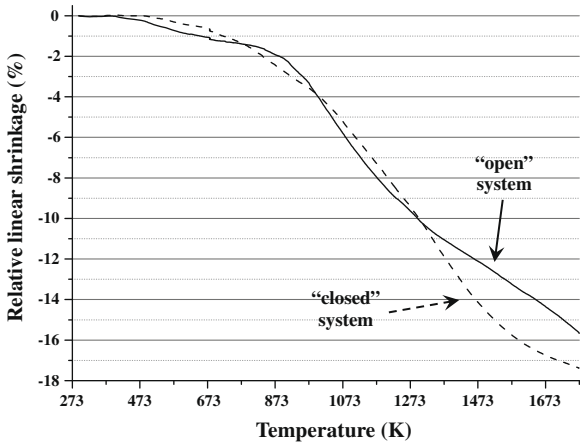

Fig. 4. Relative linear shrinkage of the $U_{0.5}Th_{0.5}O_2$ pellets versus the heat temperature for 'open' (straight) and 'closed' (dash) systems.

ical stability of the oxide phase at these temperatures. Nevertheless, two steps could be distinguished, corresponding to the major phenomena occurring during the heat treatment of the ceramic materials. The first part of the shrinkage lies between 773 and 1073 K and appears to be limited. It can be correlated to the grain growth step (driven by surface diffusion) which generally presents a lower energy of activation compared to the sintering process (driven by volume diffusion) in this range of temperature [16]. This densification step mainly takes place above 1073 K and was associated to the strong shrinkage observed up to 1773 K. At this last temperature, the sintering appears almost complete and is associated to the good densification of the samples. It is worth to note that, even if high shrinkage was obtained for both preparation routes, the maximal value was reached for the compounds prepared in 'closed system'.

The densification rate of the pellets prepared after firing the samples between 1673 and 1773 K was then studied versus the heating time (Table 2) and correlated to SEM observations. As expected, the samples obtained at 1673 K (Fig. 5(a–b)) appeared poorly densified ($83\% < d_{exp}/d_{calc} < 86\%$ for the 'closed system'), even after 10 h of heat treatment, consistently to the sintering temperature determined from dilatometric measurements. That was associated to the important porosity observed at the surface of the solid and to the weak grain growth: indeed, at this temperature, the average grain size was found to be about 5 μm, this value

Table 2
Relative densities (expressed in percentage of calculated density) of $U_{1-x}Th_xO_2$ solid solutions pellets after heating at 1673 and 1773 K.

T (K)	Heating time (h)					
	0.5	1	2	3	5	8
1673						
'Open system'	77	79	79	79	80	79
'Closed system'	82	84	86	86	86	85
1773						
'Open system'	93	96	96	99	97	97
'Closed system'	88	90	94	98	97	97

All the densities are given with an experimental uncertainty of about 2%.

being similar to that determined for the initial oxide powders. On the other hand, the samples prepared at 1773 K revealed a significant higher density (Fig. 5(c–d)). For both systems studied, the maximum value of the density was obtained after only 3 h of heating and reached 95% to 97% of the calculated value, corresponding to a global porosity lower than 5%. This densification was also evidenced through SEM experiments with the observation of several grain boundaries associated to an important grain growth (up to 20 μm). The remaining micrometric open pores were mainly detected between the grains. The extension of the heating treatment over 3 h was not associated to a higher densification, indicating that the residual porosity was not eliminated at this temperature. Nevertheless, the use of wet chemistry methods for the preparation of (U,Th) mixed dioxides allows to lower significantly the sintering temperature. Indeed, the preparation of highly densified actinide dioxide pellets is generally reported between 1873 and 1973 K in the literature [17] while lower temperatures are only mentioned for the use of an oxidative atmosphere [18,19].

Complementary experiments at 1973 K allowed to eliminate the residual intergranular open porosity. A slight increase of the densification rate was observed for both studied systems: after 10 h of heating at this temperature, the relative density was found to be almost 96% of the calculated value for the 'open system' and 98% for the 'closed system'. Even if both compounds exhibited close densification rates, they revealed some important differences in the microstructure. More particularly, the average grain size appeared considerably larger in the case of the pellets prepared by the 'closed system' (Fig. 5(f)) (up to 40–50 μm) while that initially prepared *via* 'open system' (Fig. 5(e)) revealed a heterogeneous distribution of the grain size with the presence of small particles of about 5 μm. Such small particles were only eliminated when performing hot pressing experiments.

Correlatively to the grain size, the occurrence of the grain boundaries is dependent on the way of preparation. An important quantity of grain boundaries could degrade significantly the chemical durability of the (U,Th) mixed dioxides since they are generally well-known to be preferential zones of alteration during aqueous corrosion processes [20,21]. In these conditions, the use of the 'closed system' could offer some improvements on the physico-chemical properties of interest of mixed actinide dioxides which were evaluated during leaching tests.

3.3. Evaluation of the chemical durability

The influence of the synthesis procedure on the behaviour of $U_{1-x}Th_xO_2$ sintered pellets during leaching tests was examined. In this purpose, three $U_{0.5}Th_{0.5}O_2$ samples were altered in 10^{-1}–10^{-4} M HNO_3 at 298 K: two of them were prepared from 'open system' then sintered by natural or hot pressing techniques while the third one was obtained from 'closed system' then sintered after room-temperature compaction. From a general point of view, as

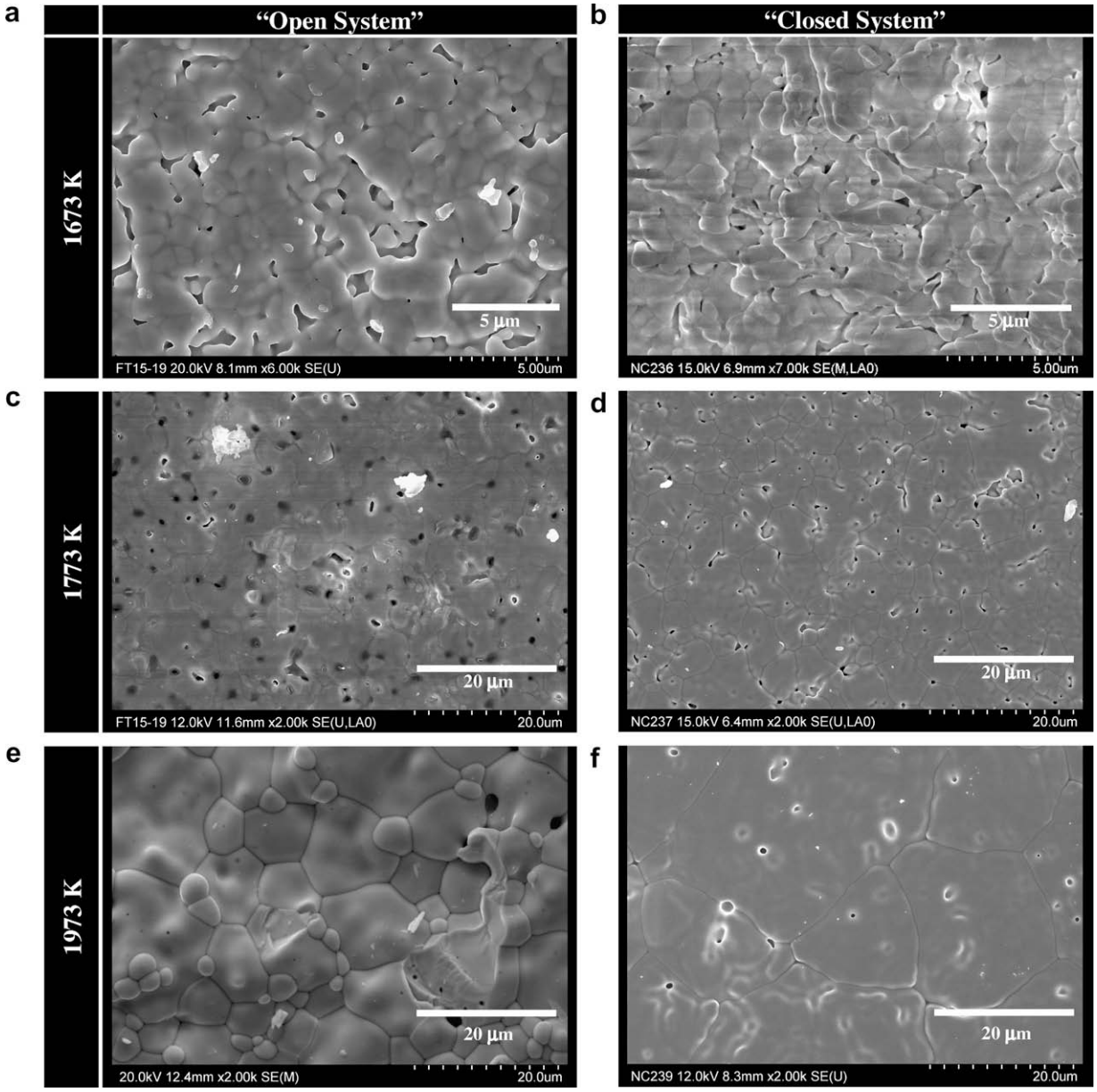

Fig. 5. SEM observations of the $U_{0.5}Th_{0.5}O_2$ sintered pellets prepared after heating at 1673, 1773 and 1973 K.

already shown in [22,23], the relative behaviour of thorium and uranium during the leaching was found to vary with the pH. In the early days of the leaching tests, a slightly higher release in actinides was observed probably due to the presence of more soluble minor phases or defects at the surface of the pellet. The normalized dissolution rates were then found to be similar for both actinides at pH 1. Consequently, the dissolution could thus be qualified as congruent $\left(1/3 \leq \frac{R_L(U)}{R_L(Th)} \leq 3\right)$. On the contrary, when increasing the pH value up to 4, the dissolution appears clearly incongruent because of the rapid precipitation of thorium as a neoformed phase [22]. For this reason, the determination of the normalized dissolution rates was based on the uranium concentration in the leachate.

The comparative evolution of the normalized weight loss, $N_L(U)$, measured in 10^{-1} M HNO_3 is shown in Fig. 6 for $U_{0.5}Th_{0.5}O_2$ pellets prepared through 'open' and 'closed' systems. In 'open system', two different pellets were sintered either at room temperature or through hot pressing experiments. The normalized dissolution rate obtained for 'open system' samples ($R_L(U) = 3 \times 10^{-4}$ g · m^2 · d^{-1}) is about one order of magnitude larger than that of 'closed system' samples ($R_L(U) = 2 \times 10^{-5}$ g · m^2 · d^{-1}). In these conditions, the improvement in the crystallization state of the precursors observed when using hydrothermal processes seems to influence the physico-chemical properties of the final compounds in terms of resistance to aqueous alteration. Nevertheless, for samples prepared from poorly-crystallized precursors, a similar dissolution rate was only obtained after a hot pressing procedure which allows to get very cohesive materials exhibiting a relative density close to 100% and a microstructure with a few grain boundaries. In these conditions, the higher grain growth of the 'closed system' compounds emphasized in the previous part could be also considered as a benefit for the chemical durability of the mixed actinide dioxides.

Finally, since uranium dioxide is known to be more soluble than thorium dioxide in oxidative media [24,25], it appeared interesting to study the effect of the chemical composition of (U,Th) mixed dioxides on the normalized dissolution rate. The logarithm of the normalized leaching rates determined at 298 K

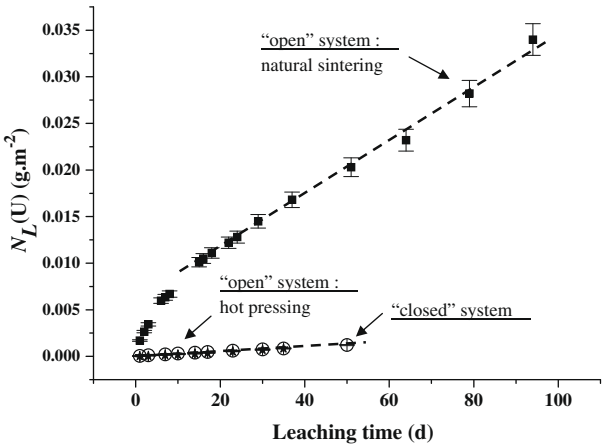

Fig. 6. Evolution of the normalized leaching N_L(U) of $U_{0.5}Th_{0.5}O_2$ (10^{-1} M HNO_3, T = 298 K) prepared from 'open system' (■ room temperature sintering/★ hot pressing) or 'closed system' (○).

in 10^{-1} M HNO_3 for several compositions of $U_{1-x}Th_xO_2$ solid solution was then plotted versus the substitution rate x. As previously observed during the study of powdered samples, the value of log (R_L) exhibits a linear variation versus x [23]. Nevertheless, this dependence appears clearly weaker for samples prepared from well crystallized low-temperature precursors probably due to the homogenization of the cations distribution expected in the structure for hydrothermal compounds thus to the absence of more soluble U-enriched zones in the solids which could increase the normalized dissolution rates [23]. Statistical EPMA experiments are now planned to confirm the better cationic distribution expected from this way of synthesis.

4. Conclusion

$U_{1-x}Th_xO_2$ sintered pellets were successively obtained from crystallized $U_{1-x}Th_x(C_2O_4)_2$. $2H_2O$ precursors precipitated at low temperature through two chemical routes. Among them, the use of hydrothermal conditions led to a significant improvement in the crystallization state correlated to important modifications of the microstructure.

The initial preparation of $U_{1-x}Th_x(C_2O_4)_2 \cdot 2H_2O$ was thus associated to the lowering of the sintering temperature since similar results are generally obtained only when heating between 1873 K and 1973 K. Moreover, the increase of the heating temperature to 1973 K led to a higher average grain size for the compounds prepared from 'closed system'.

Such modifications in the preparation method affect significantly the resistance of the materials to aqueous alteration. Indeed, the normalized dissolution rate was found to be lowered by one order of magnitude when using hydrothermal conditions for the precipitation of precursors ($R_L(U) = 2 \times 10^{-5}\ g \cdot m^{-2} \cdot d^{-1}$ in 10^{-1} M HNO_3 at 298 K). Moreover, the increase of R_L generally observed along with the substitution of thorium by uranium (IV) appears to be limited in our samples, probably due to the homogenization of the cationic distribution.

Several studies are now under progress to improve the understanding of the phenomena, especially near the solid/solution interface. Complementary dissolution tests will be undertaken in order to evaluate the influence of the microstructure on the kinetic parameters and associated data (activation energy, partial orders). A special attention will be also taken to the characterization of the neoformed phases precipitated onto the surface of the leached pellets near to saturation then their solubility constant will be evaluated.

Acknowledgments

Authors would like to thank Alain Kohler from the SCM of the University Nancy-I for the SEM micrographs. They are also grateful to Jean Aupiais and Gilles Lecoq from CEA Bruyères-le-Chatel and to Hawa Badji from CEA Saclay for their help in ICP–AES measurements.

This work was financially supported by the MATINEX Research Group (CEA/CNRS/AREVA/EDF/French Universities) included in the PACEN program.

References

[1] Generation IV Roadmap Project, in: A Technology Roadmap for Generation IV Nuclear Energy Systems, D.O.E and Generation IV Forum, 2002.
[2] M. Ichimiya, Y. Sagayama, T. Am, Nucl. Soc. 90 (2004) 46.
[3] T.R. Allen, T. Am, Nucl. Soc. 94 (2006) 799.
[4] L.K. Mansur, A.F. Rowcliffe, R.K. Nanstad, S.J. Zinkle, W.R. Corwin, R.E. Stoller, J. Nucl. Mater. 329–333 (2004) 166.
[5] G. Oudinet, I. Munoz-Viallard, L. Aufore, M.J. Gotta, J.M. Becker, G. Chiarelli, R. Castelli, J. Nucl. Mater. 375 (2008) 86.
[6] P. Buisson, PhD thesis, University Grenoble 1, GRE1-0519, 1999.
[7] B. Arab-Chapelet, S. Grandjean, G. Nowogrocki, F. Abraham, J. All. Comp. 444&445 (2007) 387.
[8] N. Clavier, N. Dacheux, G. Wallez, M. Quarton, J. Nucl. Mater. 352 (2006) 209.
[9] S. Hubert, K. Barthelet, B. Fourest, G. Lagarde, N. Dacheux, N. Baglan, J. Nucl. Mater. 297 (2001) 206.
[10] J. Rodriguez-Carvajal, Fullprof.2k V1.9c, Laboratoire Léon Brillouin CEA, Saclay, France, 2001.
[11] N. Dacheux, N. Clavier, J. Ritt, J. Nucl. Mater. 349 (2006) 291.
[12] L. Duvieubourg-Garela, N. Vigier, F. Abraham, S. Grandjean, J. Solid State Chem. 181 (2008) 1899.
[13] L. Vegard, Z. Phys. 5 (1921) 17.
[14] R.D. Shannon, Acta Cryst. A32 (1976) 751.
[15] N. Vigier, S. Grandjean, B. Arab-Chapelet, F. Abraham, J. All. Comp. 444&445 (2007) 594.
[16] D. Bernache-Assollant, In Physico-Chimie du Frittage, Hermès, Paris, 1993.
[17] T.R.G. Kutty, P.V. Hedge, K.B. Khan, T. Jarvis, A.K. Sengupta, S. Majumdar, H.S. Kamath, J. Nucl. Mater. 335 (2004) 462.
[18] C.Y. Joung, S.C. Lee, S.H. Kim, H.S. Kim, D.S. Sohn, J. Nucl. Mater. 375 (2008) 209.
[19] X.D. Yang, J.C. Gao, Y. Wang, X. Chang, Trans. Nonferrous Met. Soc. China 18 (2008) 171.
[20] N. Clavier, E. du Fou de Kerdaniel, N. Dacheux, P. le Coustumer, R. Podor, J. Ravaux, E. Simoni, J. Nucl. Mater. 349 (2006) 304.
[21] E. du Fou de Kerdaniel, N. Clavier, N. Dacheux, O. Terra, R. Podor, J. Nucl. Mater. 362 (2007) 451.
[22] G. Heisbourg, S. Hubert, N. Dacheux, J. Purans, J. Nucl. Mater. 335 (2004) 5.
[23] G. Heisbourg, S. Hubert, N. Dacheux, J. Ritt, J. Nucl. Mater. 321 (2003) 141.
[24] I. Grenthe, Chemical Thermodynamics of Uranium, OECD Nuclear Energy Agency, Paris, 1992.
[25] A.S. Kertes, R. Guillaumont, Nucl. Chem. Waste Man. 5 (1985) 215.